# SLIDING MODE VECTOR CONTROL OF PMSM DRIVES WITH FLEXIBLE COUPLINGS IN MOTION CONTROL

S J Dodds, J Vittek*
*Control Research Group, *Visiting Professor to SCoT.*
stephen.dodds@spacecon.co.uk; s.j.dodds@uel.ac.uk; Jan.Vittek@fel.uniza.sk

**Abstract:** A new control system for permanent magnet synchronous motor electric drives with a significant torsion vibration mode in the mechanical coupling is presented based entirely on sliding mode principles to achieve robustness against external load torques and parametric modelling uncertainties. The user is only required to provide the demanded position and specify the settling time, no controller tuning being necessary. The vector control condition of keeping the direct axis current component approximately zero is satisfied as well as controlling either the rotor or load position to follow the demanded position with prescribed closed loop dynamics. To avoid control chatter, a boundary layer is introduced by replacing the relay control switching transfer characteristic (signum function) by a high gain having the same control saturation limits. Any steady state errors with a constant demanded rotor angle due to the finite value of the aforementioned gain are eliminated by means of an outer integral control loop. The simulations predict that the desired robustness will be achieved.

## 1. Introduction:

### 1.1. Overview:

The main contribution is a simple sliding mode controller that simultaneously achieves vector control and position control with prescribed closed loop dynamics for a permanent magnet synchronous motor (PMSM) drive with a mechanical load that may contain a significant vibration mode, and without the need for any knowledge of the motor or load parameters. This robustness is achieved using the sliding mode control (SMC) described by Utkin, 1992. It has already been used for PMSM position control by Aguilar, 2002, Lee et. al., 1994, and Vittek and Dodds, 2003, assuming the moving mechanism obeys rigid body dynamics. The combination of the elasticity and the inertia of the materials used in controlled mechanisms, however, gives rise to vibration modes that, if ignored, can impair control accuracy and some progress on their active control has already been made. For PMSM drives containing a single torsion vibration mode, SMC has been applied in an outer loop by Dodds and Vittek, 2007, and directly by Hace, et. al., 2005. The control system offered here, however, is unique in requiring no tuning when commissioning and yielding a closed loop step response with a prescribed settling time using the formula of Dodds, 2008.

### 1.2. Introduction to Sliding Mode Control:

Sliding mode control (Utkin, 1992) is well known to achieve robustness. Fig. 1 shows the general block diagram for a single input, single output (SISO) plant. Here, $\mathbf{x} \in \Re^n$, is the state vector, where n is the order of the plant, and $\mathbf{y} = \in \Re^{r-1}$, where $y_i = d^i y / dt^i$ and r is the relative degree (or rank) of the plant such that the $r^{th}$ output derivative is $y^{(r)} = h_r(\mathbf{x}, u)$ and is *not* a state variable because of its dependence on the control input, u. The

elements of **y** are all state variables, their equations shown in Fig. 1 constituting a transformation to a new set of state variables. The SMC law is a bang-bang state feedback control law where $u = \pm U$, switching

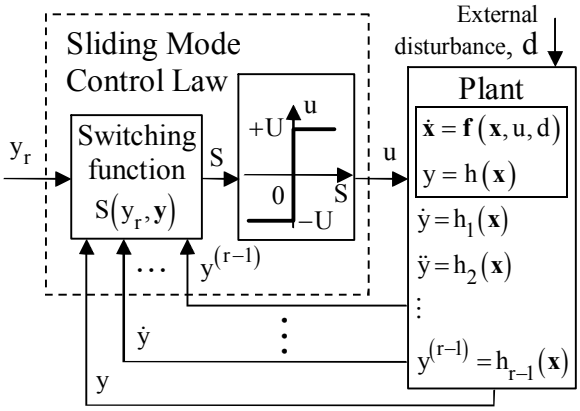


Fig. 1. Basic SISO sliding mode control.

whenever S passes through zero. The switching function, $S(y_r, \mathbf{y})$, is designed such that over the normal range of operating states, u is switched to the value that drives **y** towards the switching boundary,

$$S(y_r, \mathbf{y}) = 0 \Rightarrow S\left(y_r, y, \dot{y}, \cdots y^{(r-1)}\right) = 0 \quad (1)$$

from both sides as shown in Fig. 2 for $r = 2$.

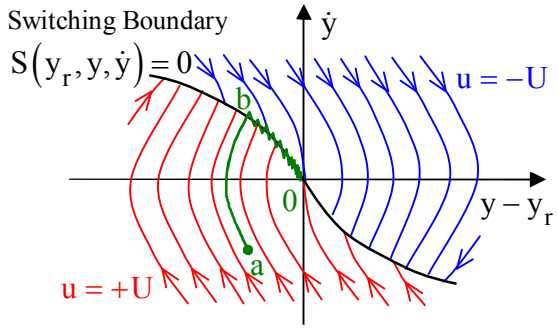


Fig. 2. A closed loop phase portrait and trajectory

With an arbitrary starting point, a, the state trajectory at first moves towards the switching boundary under control saturation and upon crossing the boundary at point, b, **y** is held on the boundary due to u rapidly switching between $+U$ and $-U$, in theory at an infinite frequency and with a continuously varying mark-space ratio. Then the trajectory zigzags about but remains in a close neighbourhood of the switching boundary. On a larger scale it appears to *slide* in the surface and the system is said to be operating in a sliding mode. Also, during this sliding motion, Eq. (1) is, in theory, obeyed and becomes the closed loop differential equation. If the switching boundary is linear, i.e.,

$$y_r - \left(y + q_1\dot{y} + q_2\ddot{y} + \ldots + q_{r-1}y^{(r-1)}\right) \quad (2)$$

where $q_i$, $i = 1, 2, \ldots, r-1$, are constant coefficients that may be chosen to yield the desired closed loop dynamics, then the closed loop system has the transfer function

$$\frac{y(s)}{y_r(s)} = \frac{1}{1 + sq_1 + s^2q_2 + \ldots + s^{r-1}q_{r-1}} \quad (3)$$

which is independent of the plant parameters and the external disturbance, indicating extreme robustness. Sliding motion can only be sustained over a finite region of the switching boundary, some trajectories being directed away from the boundary outside this region. In general, however, the sliding region may be increased by increasing the maximum control level, U, provided this is practicable.

If the plant is of full rank, then $r = n$ and $\mathbf{y} = \left[y\ \dot{y} \cdots y^{(r-1)}\right]^T$ is a complete state vector, enabling *complete* control of the plant. If, however, the plant is not of full rank, i.e., $r < n$, which is the case when controlling the rotor position of the PMSM drive with the flexible coupling, then the sliding mode control law can only control a *subsystem* of the plant with the state variables, $y_r, y, \dot{y}, \cdots y^{(r-1)}$. In this case, there exists an uncontrolled subsystem of order, $n - r$. The dynamics of this uncontrolled subsystem is referred to as the *zero dynamics*.

## 2. Model of the Controlled Plant:

The complete model of the PMSM and its mechanical load is given here as it is used for the simulations and the relative degree determinations. The state differential equations of the PMSM are:

$$di_d/dt = -Ai_d + B\omega_r i_q + Fu_d \quad (4)$$

$$di_q/dt = -\left(Ci_d + E\right)\omega_r - Di_q + Gu_q \quad (5)$$

$$d\omega_r/dt = M\left(\Gamma_c - \Gamma_{Lr}\right) \quad (6)$$

$$d\theta_r/dt = \omega_r \quad (7)$$

in the synchronously rotating d-q co-ordinate system, where $i_d$, $i_q$ are the stator current vector components, $u_d$, $u_q$ are the voltage vector components, which are also the control variables, $\omega_r$ and $\theta_r$ are the rotor angular velocity and angle, $\Gamma_c$ is the electromagnetic torque given by

$$\Gamma_c = J_r\left(H + Ki_d\right)i_q \quad (8)$$

and $\Gamma_{Lr}$ is the total load torque acting on the rotor given by

$$\Gamma_{Lr} = \Gamma_{Lre} + \Gamma_{Ls} \quad (9)$$

where $\Gamma_{Lre}$ is an external load torque applied directly to the rotor and $\Gamma_{Ls}$ is the load torque presented by the driven mechanical load, which in this case is the torsion torque of the flexible drive shaft. The constant coefficients are:

$$\begin{cases} A = R_s/L_d;\ B = pL_q/L_d;\ C = pL_d/L_q; \\ D = R_s/L_q;\ \ E = p\Psi_{PM}/L_q;\ F = 1/L_d; \\ G = 1/L_q;\ H = 3p\Psi_{PM}/\left(2J_r\right); \\ K = 3p\left(L_d - L_q\right)/\left(2J_r\right);\ M = 1/J_r \end{cases}$$

where $\Psi_{PM}$ is the permanent magnet flux, $R_s$ is the stator resistance, $L_d$ and $L_q$ are the direct and quadrature axis inductances, p is the number of pole pairs and $J_r$ is the rotor moment of inertia.

The driven mechanism is a balanced mass with moment of inertia, $J_L$, coupled to the motor shaft via a torsion spring with spring constant, $K_s$, as shown in Fig. 3(a).

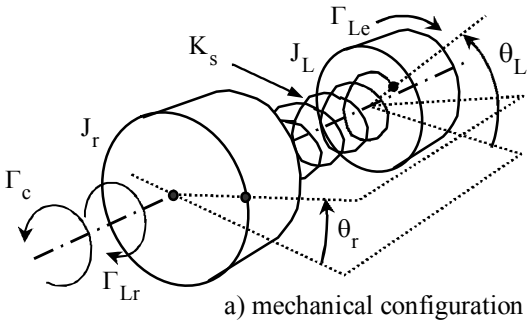


a) mechanical configuration

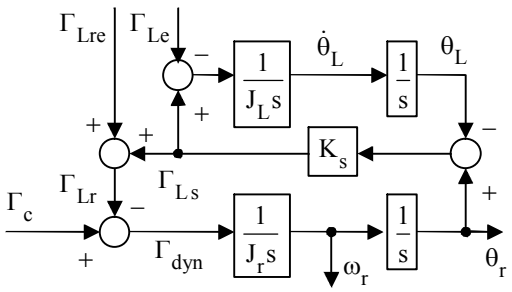


b) block diagram

Fig 3. State variable block diagram model of the driven mechanism.

The corresponding torque balance equations are as follows:

$$J_r\ddot{\theta}_r = \Gamma_c - \Gamma_{Lre} + K_s\left(\theta_L - \theta_r\right) \quad (10)$$

$$J_L\ddot{\theta}_L = K_s\left(\theta_r - \theta_L\right) - \Gamma_{Le} \quad (11)$$

where $\theta_r$ is the rotor angle, $\theta_L$ is the load mass angle, $\Gamma_{Lre}$ and $\Gamma_{Le}$ are the external load torques applied, respectively, to the rotor and the load mass.

The state variable block diagram of Fig. 3(b) follows from Eq. (10) and Eq. (11). The

dynamic (i.e., inertial) torque, $\Gamma_{dyn} = J_r \dot{\omega}_r$, is shown on this diagram.

Fig. 4 shows the main hardware elements of the controlled plant together with the inverse and forward Clark-Park transformations, which are the same as for other vector control schemes and implemented on a digital processor. The subscript 'dem'

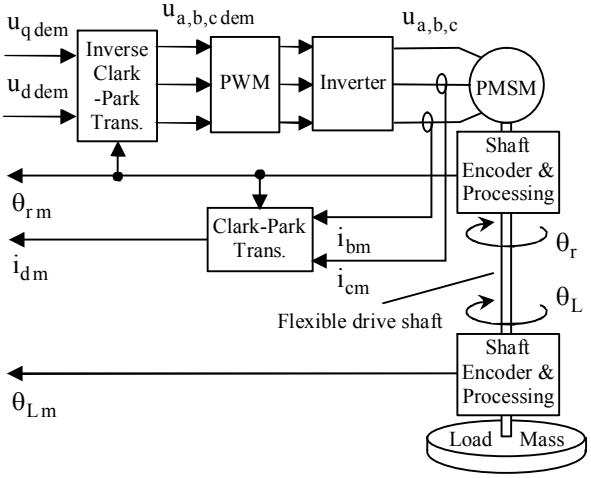


Fig. 4. Overall block diagram of the plant.

indicates a 'demanded value' and the subscript, 'm', indicates a measured value. Details of the pulse width modulation (PWM) scheme are not given here as it is a standard one. It is sufficient to state that the stator voltages, $u_a$, $u_b$ and $u_c$, are switched between the power supply voltage levels such that their short-term mean values are equal, respectively, to the demanded values, $u_{a\,dem}$, $u_{b\,dem}$ and $u_{c\,dem}$, which are generated from the demanded direct axis and quadrature axis stator voltage vector components, $u_{d\,dem}$ and $u_{q\,dem}$ via the inverse Clark-Park transformation as shown in Fig. 3. To summarise, the two control variables are $u_{d\,dem}$ and $u_{q\,dem}$, one controlled variable is $i_{d\,m}$ and the other controlled variable is either $\theta_{L\,m}$ or $\theta_{r\,m}$.

# 3. Sliding Mode Control Design:

## 3.1. Relative Degrees of Plant:

The relative degree of a plant with respect to a given controlled output is the lowest derivative of that output with respect to time that has direct algebraic dependence on any control variable. It is found by repeatedly differentiating the measurement equation and substituting for the derivatives of any state variables that appear on the right hand side of the resulting equations, using the state differential equations.

In the following, the relative degrees with respect to the controlled outputs, $i_d$, $\theta_r$ and $\theta_L$ are derived as these are assumed to be the same as those with respect to the measurements, $i_{d\,m}$, $\theta_{r\,m}$ and $\theta_{L\,m}$.

**3.1.1. Relative degree with respect to $i_d$:** By inspection of Eq. (4), $di_d/dt$ has direct algebraic dependence on $u_d$ and therefore the relative degree is

$$r_i = 1 \qquad (12)$$

**3.1.2. Relative degree with respect to $\theta_r$:** By inspection of Eq. (10), $\ddot{\theta}_r$ has no direct algebraic dependence on $u_d$ or $u_q$, so making $\ddot{\theta}_r$ the subject of the equation and substituting for $\Gamma_c$ using (8) yields:

$$\ddot{\theta}_r = \left(H + Ki_d\right)i_q + M\left[K_s\left(\theta_L - \theta_r\right) - \Gamma_{Lre}\right] \qquad (13)$$

Since only state variables and external disturbances appear on the RHS of Eq. (13), this equation is differentiated and substitutions made for $di_d/dt$ and $di_q/dt$ using Eq. (4) and Eq. (5) yielding:

$$\begin{aligned}\dddot{\theta}_r &= \left(H + Ki_d\right)\frac{di_q}{dt} + Ki_q\frac{di_d}{dt} \\ &\quad + M\left[K_s\left(\dot{\theta}_L - \dot{\theta}_r\right) - \dot{\Gamma}_{Lre}\right] \Rightarrow \\ \dddot{\theta}_r &= \left(H + Ki_d\right)\left[-\left(Ci_d + E\right)\omega_r - Di_q + Gu_q\right] \\ &\quad + Ki_q\left[-Ai_d + B\omega_r i_q + Fu_d\right] \\ &\quad + M\left[K_s\left(\dot{\theta}_L - \dot{\theta}_r\right) - \dot{\Gamma}_{Lre}\right] \qquad (14)\end{aligned}$$

Since, $\dddot{\theta}_r$ has direct algebraic dependence on both $u_d$ and $u_q$, the relative degree is

$$r_r = 3 \qquad (15)$$

**3.1.3. Relative degree with respect to $\theta_L$.** By inspection of Eq. (11), $\ddot{\theta}_L$ has no direct algebraic dependence on $u_d$ or $u_q$, so making $\ddot{\theta}_L$ the subject of the equation and differentiating yields:

$$\dddot{\theta}_L = \left[K_s\left(\dot{\theta}_r - \dot{\theta}_L\right) - \dot{\Gamma}_{Le}\right]/J_L \qquad (16)$$

$\dot{\theta}_r$ and $\dot{\theta}_L$ are state variables and therefore $\dddot{\theta}_L$ has no direct algebraic dependence on $u_d$ or $u_q$. Differentiating Eq. (16) yields:

$$\ddddot{\theta}_L = \left\{K_s\left[\ddot{\theta}_r - \ddot{\theta}_L\right] - \ddot{\Gamma}_{Le}\right\}/J_L \qquad (17)$$

According to Eq. (13) and Eq. (11), there is no direct algebraic dependence of $\ddot{\theta}_r$ or $\ddot{\theta}_L$, and hence $\ddddot{\theta}_L$ given by Eq. (17), on $u_d$ or $u_q$. So Eq. (17) is differentiated and substitutions made for $\dddot{\theta}_r$ and $\dddot{\theta}_L$ using Eq. (14) and Eq. (16):

$$\begin{aligned}\ddddot{\theta}_L &= M'\left\{K_s\left[\dddot{\theta}_r - \dddot{\theta}_L\right] - \dddot{\Gamma}_{Le}\right\} \\ &= M'\left\{K_s\left[\begin{bmatrix}\left(H + Ki_d\right)\begin{bmatrix}-\left(Ci_d + E\right)\omega_r \\ -Di_q + Gu_q\end{bmatrix} \\ +Ki_q\left[-Ai_d + B\omega_r i_q + Fu_d\right] \\ +M\left[K_s\left(\dot{\theta}_L - \dot{\theta}_r\right) - \dot{\Gamma}_{Lre}\right]\end{bmatrix}\right] - \dddot{\Gamma}_{Le}\right\} \\ &\quad \begin{bmatrix}-\left[K_s\left(\dot{\theta}_r - \dot{\theta}_L\right) - \dot{\Gamma}_{Le}\right]/J_L\end{bmatrix}\end{aligned} \qquad (18)$$

The direct algebraic dependence of $\dddot{\theta}_L$ on $u_d$ and $u_q$ is now apparent and therefore the relative degree is

$$r_L = 5 \qquad (19)$$

### 3.2. The Settling Time Formula:

The sliding mode controllers for the three controlled outputs will be designed to yield linear closed loop dynamics with non-overshooting step responses to 95% of the steady state outputs using the settling time formula of Dodds (2008). The sliding surfaces will be hyper-planes in the output derivative state sub-space yielding linear closed loop systems with coincident poles at $s_{1,2,\ldots,n} = -1/T_c$ and the corresponding settling time formula is:

$$T_s = 1.5\left(1 + n\right)T_c \qquad (20)$$

### 3.3. Individual Sliding Mode Control Loops:

Fig. 5 shows the overall control system block diagram with the three sliding mode controllers.

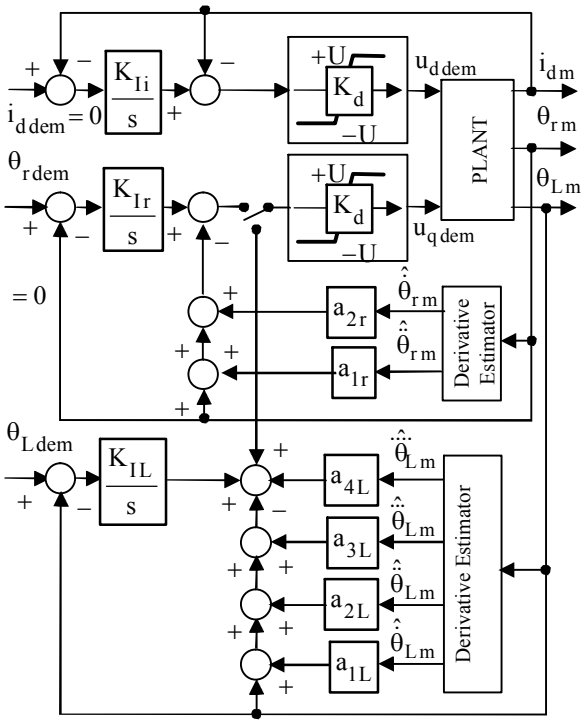


Fig 5. Overall control system block diagram.

Let $T_{si}$, $T_{sr}$ and $T_{sL}$ be, respectively, the required settling times of the direct axis stator current, rotor angle and load mass angle control loops. Then equating the characteristic polynomials obtained from Fig. 5 to the corresponding desired characteristic polynomials obtained using settling time formula of Eq. (20) yields the controller parameters, as follows:

For the direct axis stator current control loop, $r_i = 1$, so no output derivatives are needed according to section 1.2. Then

$$1+\frac{1}{K_{Ii}}s = 1+\frac{T_{si}}{3}s \Rightarrow \boxed{K_{Ii}=\frac{3}{T_{si}}} \qquad (21)$$

For the rotor angle control loop, $r_r = 3$ and therefore the first and second output derivatives are needed. In this case:

$$1+\frac{1}{K_{Ir}}\left(s+a_{1r}s^2+a_{2r}s^3\right)=\left(1+\frac{T_{sr}}{6}s\right)^3$$
$$=1+3.\frac{T_{sr}}{6}s+3.\left(\frac{T_{sr}}{6}\right)^2 s^2+\left(\frac{T_{sr}}{6}\right)^3 \Rightarrow$$

$$\boxed{K_{Ir}=\frac{2}{T_{sr}},\quad a_{1r}=\frac{T_{sr}}{6},\quad a_{2r}=\frac{T_{sr}^2}{108}} \qquad (22)$$

For the load mass angle control loop, $r_L = 5$ and therefore all the output derivatives up to order, 4, are needed. So

$$1+\frac{1}{K_{IL}}\left(s+a_{1L}s^2+a_{2L}s^3+a_{3L}s^4+a_{5L}s^5\right)$$
$$=\left(1+\frac{T_{sL}}{9}s\right)^5=1+5.\frac{T_{sL}}{9}s+10.\frac{T_{sL}^2}{81}s^2$$
$$+10.\frac{T_{sL}^3}{729}s^3+5.\frac{T_{sL}^4}{6561}s^4+\frac{T_{sL}^5}{59049}s^5 \Rightarrow$$

$$\boxed{K_{IL}=\frac{9}{5T_{sL}},\quad a_{1L}=\frac{10T_{sL}}{45},\ a_{2L}=\frac{10T_{sL}^2}{405},\ a_{3L}=\frac{T_{sL}^3}{729},\ a_{4L}=\frac{T_{sL}^4}{32805}} \qquad (23)$$

The $i_d$ control loop is operated permanently but, of course, either the $\theta_r$ or the $\theta_L$ control loop is operated, according to the switch position in Fig. 5. It should be noted that the term, $B\omega_r i_q$, in Eq. (4) behaves like a disturbance input to the $i_d$ SMC loop and is counteracted by this loop while $i_d$ is driven approximately to zero. This minimises the interaction in the plant, as can be seen by inspection of Eq. (5), Eq. (6) and Eq. (8) after setting $i_d = 0$. Hence the plant, although it is a multivariable one, i.e., more than one control input and more than one controlled output, can be controlled effectively by two separate single input, single output sliding mode controllers.

The output derivative estimation may be implemented by various algorithms some of which incorporate measurement noise filtering but in the simulations to follow ideal differentiation is assumed.

## 4. Simulations:

The parameters of the non-salient PMSM are: winding resistance: $R_s = 33.3\Omega$; winding inductances: $L_d = L_q = 53.8\,\text{mH}$; permanent magnet flux: $\Psi_{PM} = 0.262$ Wb; number of pole pairs: $p = 3$; rotor moment of inertia: $J_r = 0.0003\ \text{Kg m}^2$.

The parameters of the driven mechanical load are as follows: Load mass moment of inertia: $J_L = 0.0003\ \text{Kg m}^2$; shaft torsion spring constant: $K_s = 9\ \text{Nm rad}^{-1}$.

The controller parameters are as follows: Settling times: $T_{si} = T_{sr} = T_{sL} = 0.2\,\text{s}$; saturation element gain: $K = 1500$ and 4444, respectively for rotor angle and load angle control; Control saturation limit: $U = 360\,\text{V}$. In all the simulation results presented, $\Gamma_{Lre} = 0$ and the external load torque, $\Gamma_{Le}$, applied to the load mass ramps from zero value at a constant rate of 20 Nm/s to a maximum value of 2 Nm and stays at this value. This is applied about half way through each run of 1 second duration.

First, simulations of the rotor control are presented with a step angle demand of $\theta_{rdem} = 10\,\text{rad}$ and zero initial conditions. Fig. 6 shows the rotor angle response, $\theta_r(t)$, compared with the ideal step response, $\theta_{rid}(t)$, of the system with transfer function:

$$\frac{\theta_{rid}(s)}{\theta_{rdem}(s)} = \left[1/\left(1 + s\,T_{sr}/6\right)\right]^3 \qquad (24)$$

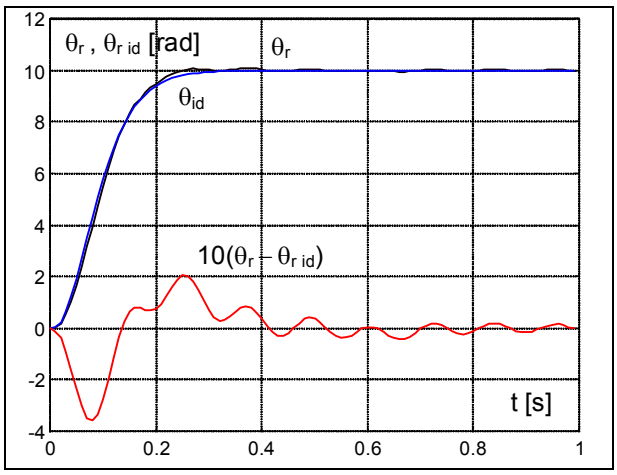


Fig. 6. Rotor control: ideal and real rotor angles.

The simulated real response follows the ideal one relatively closely on the scale of 10 rad., but the peak transient error of about 0.2 rad. is significant. The external load torque, however, has a negligible effect and this is attributed to the 'cushioning' effect of the torsion spring characteristic of the drive shaft. The oscillations are movements of the rotor produced by the load torque, $\Gamma_{Ls}(t)$, acting on the rotor due to the oscillating, uncontrolled load mass. This occurs due to the need for the gain, K, to be finite.

Fig. 7 shows the corresponding load mass angle response indicating the oscillatory zero dynamics of the system. The non-zero error between the mean value of $\theta_r$ and $\theta_L$ in the steady state is torsional deflection angle of the shaft due to counteraction of $\Gamma_{Le}$.

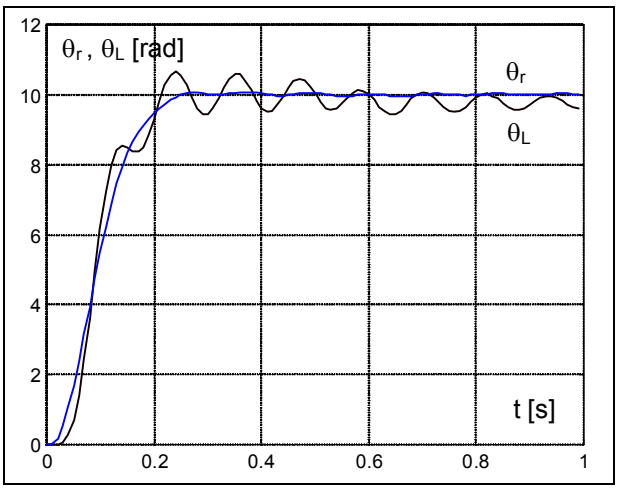

Fig. 7. Rotor control: load mass angle.

Next, a simulation of the load mass angle control is presented. Fig. 8 shows the rotor angle response, $\theta_L(t)$, compared with the step response, $\theta_{Lid}(t)$, of the ideal closed loop system with transfer function:

$$\frac{\theta_{Lid}(s)}{\theta_{Ldem}(s)} = \left[1/\left(1+sT_{sL}/6\right)\right]^5 \qquad (25)$$

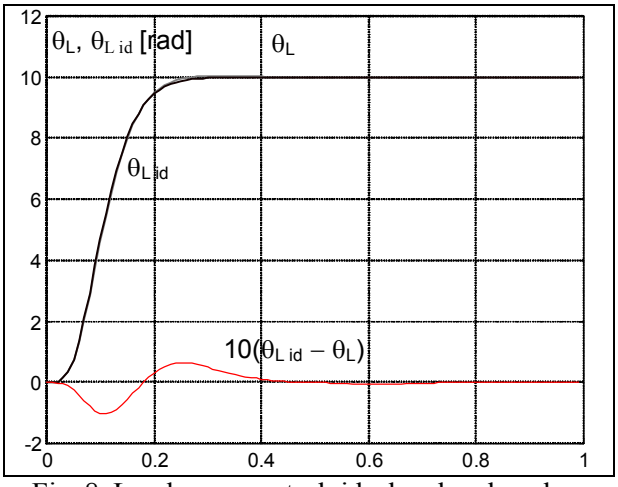

Fig. 8. Load mass control: ideal and real angles.

The peak transient error is hardly visible on the scale of 10 rad. and is seen to be about 0.1 rad on the magnified error plot. The effect of the external load torque is negligible thanks to the robustness of SMC.

Fig. 9 shows the corresponding rotor angle response, which exhibits no oscillations

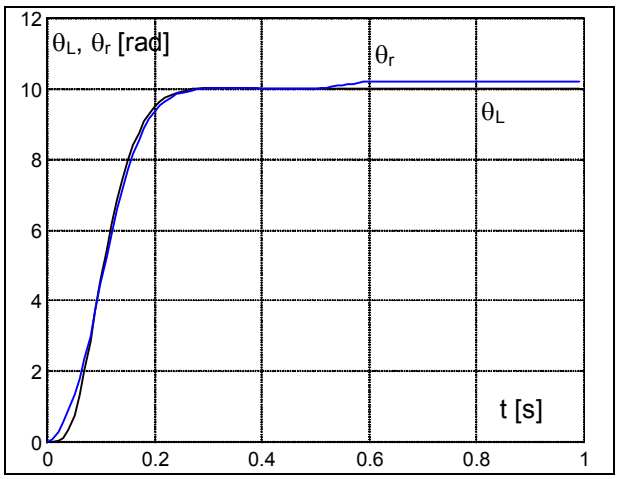

Fig. 9. Load mass control: rotor angle.

because the SMC exercises full state control without zero dynamics in this case. The steady state error between $\theta_r$ and $\theta_L$, which is the torsional deflection angle of the shaft due to counteraction of $\Gamma_{Le}$, is clearly visible.

## 5. Acknowledgement:

The authors wish to thank the Slovak Grant Agency VEGA for funding the project No.4087/07 'Servosystems with Rotational and Linear Motors without Position Sensor'.

## 6. Conclusions and Recommendations:

The simulations predict that the proposed sliding mode control system can be made to follow the ideal closed loop dynamics with moderate accuracy, for both rotor angle control and load mass angle control. As a preliminary result, this is acceptable considering that no motor or driven load parameters were needed. The vector control condition of keeping the direct axis current to small proportions is very effectively maintained.

It is recommended that the potential accuracy is ascertained by exploring the limits of the sampling frequency and the saturation element gain. The limitations of various derivative

estimation algorithms and the effects of measurement noise should also be explored .

An interesting new line of investigation would be the application of the new SMC system to mechanical loads containing more than one significant vibration mode.

The results obtained here are sufficiently promising to warrant experimental trials, which will attract potential industrial users.

## 7. References:

Aguilar, O., Loukianov, A. G., Canedo, J. M., "Observer-based Sliding Mode Control of Synchronous Motor", *Proceedings of IFAC Congress on Automatic Control*, Guadalajara, Mexico 2002, CD-Rom.

Dodds, S. J., "Settling time formulae for the design of control systems with linear closed loop dynamics", *Proceedings of AC&T 2008*, SCOT, University of East London, UK, ISBN 0-9550008-5-8.

Dodds, S. J., Vittek, J., "Sliding mode control of PMSM Electric Drives with Flexible Coupling", *Proceedings of EDPE 2007*, Portoroz, Slovenia, CD-Rom.

Hace, A., Jezernik, K., Sabanovic, A., "Improved Design of VSS Controller for a Linear Belt-Driven Servomechanism", *IEEE/ASME Trans. on Mechatronics*, Vol. 10, no.4, pp 385-390, 2005.

Lee, J. H., Ko, J. S., Chung, S. K., Lee D. S., Lee, J. J., Young M. J, "Continuous Variable Structure Controller for BLDSM Position Control with Prescribed Tracking Performance", *IEEE Trans. on Industrial Electronics*, Vol. 41, No. 5, Oct. 1994.

Utkin, V. I., *Sliding Modes in Control Optimization*, Springer-Verlag, 1992, ISBN 9780387535166.

Vittek, J. Dodds, S. J., *Forced Dynamic Control of Electric Drives*, Research Monograph, University of Zilina Press, 2003, ISBN 80-8070-087-7.